Mapping Sea Grass Coverage of Tanjung Benoa Bali Using Medium Resolution Satellite Imagery Sentinel 2B

(Pemetaan Liputan Rumput Laut Tanjung Benoa Bali Menggunakan Imejan Satelit Resolusi Sederhana Sentinel 2B)

ZAINUL HIDAYAH[1,*], LUCAS DE OLIVEIRA VIEIRA[2], RAHMA SAFITRI[1], HERLAMBANG AULIA RACHMAN[1] & ABDUR RAHMAN AS-SYAKUR[3,4]

[1]Department of Marine Science and Fisheries, Faculty of Agriculture, Universitas Trunojoyo Madura, Raya Telang 02 Madura East Java, Indonesia
[2]Laboratory of Systematics and Ecology of Aquatic Organisms, Centre of Agrarian and Environmental Sciences, Federal University of Maranhão, Chapadinha, State of Maranhão, Brazil
[3]Department of Marine Science, Faculty of Marine and Fisheries, Universitas Udayana Bukit Jimbaran Campus Bali, Indonesia
[4]Environmental Research Centre, Universitas Udayana, Denpasar Bali, Indonesia

ABSTRACT

Seagrass beds are important components of a coastal ecosystem. This ecosystem serves as the primer producers of the water food chain, habitat for marine biota, produces organic carbon, and indirectly contributes to the economic well-being of coastal communities. However, the ecosystem is vulnerable to damage caused by natural factors and human activities. The objectives of this study were, firstly to identify the distribution of seagrass beds in Tanjung Benoa using Sentinel 2B satellite imagery and secondly to compare classification results from two different approaches namely pixel-based image classification and object-based image classification. Accuracy-test was carried out using field data reference of 195 sample points in the form of a 10 m X 10 m transect. The image pre-processing process was conducted with Bottom of Atmosphere (BoA) correction using the Dark Object Subtraction (DOS) method. Furthermore, the water column correction was performed using the Depth Invariant Index (DII) and the Lyzenga algorithm. The mapping results showed that the area of seagrass beds in the shallow waters of Tanjung Benoa reaches 242.99 ha. There were seven seagrass species in the study area, with an average cover of 75%. The accuracy of object-based image classification was higher than that of pixel-based classification with a difference up to 25% for six classes classification and 15% for two classes classification. Excellent results for classifying seagrasses based on cover density can be obtained when high-resolution satellite imagery and OBIA are combined with the SVM or Fuzzy Logic algorithm.

Keywords: Image classification; seagrass beds; Sentinel 2B; Tanjung Benoa; water column correction

ABSTRAK

Hamparan rumput laut adalah komponen penting dalam ekosistem pantai. Ekosistem ini berfungsi sebagai pengeluar primer rantai makanan air, habitat biota marin, menghasilkan karbon organik dan secara tidak langsung menyumbang kepada kesejahteraan ekonomi komuniti pesisir. Walau bagaimanapun, ekosistem terdedah kepada kerosakan yang disebabkan oleh faktor semula jadi dan aktiviti manusia. Objektif kajian ini adalah, pertama untuk mengenal pasti taburan hamparan rumput laut di Tanjung Benoa menggunakan imej satelit Sentinel 2B dan kedua untuk membandingkan hasil pengelasan daripada dua pendekatan berbeza, iaitu pengelasan imej berasaskan piksel dan pengelasan imej berasaskan objek. Ujian ketepatan dijalankan dengan menggunakan rujukan data lapangan daripada 195 titik sampel dalam bentuk transek 10 m × 10 m. Proses pra-pemprosesan imej dijalankan berdasarkan pembetulan Bottom of Atmosphere (BoA) dengan menggunakan kaedah Dark Object Subtraction (DOS). Tambahan pula, pembetulan lajur air turut dilakukan dengan menggunakan Indeks Invarian Kedalaman (DII) dan algoritma

Lyzenga. Hasil pemetaan menunjukkan bahawa keluasan hamparan rumput laut di perairan cetek Tanjung Benoa mencapai 242.99 ha. Terdapat tujuh spesies rumput laut di kawasan kajian dengan purata penutupan 75%. Ketepatan pengelasan imej berasaskan objek adalah lebih tinggi berbanding pengelasan berasaskan piksel dengan perbezaan sehingga 25% untuk pengelasan enam kelas dan 15% untuk pengelasan dua kelas. Keputusan yang baik untuk mengelaskan rumput laut berdasarkan kepadatan penutup boleh diperoleh apabila imej satelit resolusi tinggi dan OBIA digabungkan dengan algoritma SVM atau Fuzzy Logic.

Kata kunci: Hamparan rumput laut; pembentulan kolum air; pengelasan imej; Tanjung Benoa; Sentinel 2B

INTRODUCTION

Seagrass is a typical ecosystem of tropical waters with important ecological functions for the coastal environment. The ecosystems provide critical tasks such as being the principal source of primary production, creating organic matter, and providing habitat for various marine biota with a high economic value (Ambo-Rappe et al. 2021; Manik & Apdillah 2020; Traganos et al. 2018). Around 360 fish species, 117 macroalgae species, 24 crustacean species, and 45 echinoderm species can be found in seagrass beds (Supriyadi, Iswari & Suyarso 2018). The ecosystem also serves as a spawning ground for various types of fish, supporting fisheries production and as well as mangrove ecosystem storing blue carbon stocks globally (Hidayah, Rachman & As-Syakur 2022; Unsworth, Nordlund & Cullen-Unsworth 2019). Additionally, it serves as a habitat and feeding area for endangered species such as dugongs and turtles (Cullen-Unsworth et al. 2018).

Seagrass is a flowering plant or angiosperms in shallow marine waters. Its structure is the same as land plants with roots, rhizomes, leaves, and flowers. It can grow in the mid-intertidal area to a depth of 0.5–10 m and is mostly found in the sublittoral area. The capacity to develop in a marine environment is the outcome of adaptation to high salinity conditions (Ambo-Rappe et al. 2021). Seagrass may also establish roots in the substrate to act as anchors and grow in a wet environment due to its hydrophilus adaptation. Moreover, it forms an expanse consisting of one species or more called a seagrass bed. More species are found in the tropics than in the sub-tropics, and one of the countries having the richest seagrass species in the world is Indonesia, with 13 out of 58 species (Short et al. 2007).

The seagrass beds in Indonesia are estimated at 3,000,000 ha (Unsworth et al. 2018). The area calculation carried out by the National Oceanographic Research Center obtained more detailed results, reaching 2.934.600 ha with an estimated 97.05% spread over the eastern part (Sjafrie et al. 2018). Based on these data, Indonesia accounts for approximately 18.29% of the total area of seagrass in the world (Mckenzie et al. 2020). The condition of seagrass beds in Indonesia can be categorized into three classes, namely good (43%), moderate (50%), and damaged (7%). Damage to seagrass ecosystems results from changes in environmental conditions mostly due to coastal development, coastal and land reclamation, coral and sea sand mining, and waste disposal (Fortes et al. 2018; Unsworth et al. 2018). However, the real impact of the damage is the decrease in the diversity of marine life due to the decline in the ecological function of the ecosystem (Saraswati et al. 2021). The decline in the diversity of biota also impacts the fishing activities of coastal communities, namely an increase in the operational costs of fishermen. Moreover, damage to seagrass can impact the balance of CO_2 and O_2 in the atmosphere due to the disturbance of the photosynthesis process.

Information on the distribution of tropical coastal ecosystems can be obtained by analyzing satellite imagery data (Brown et al. 2018; León-Pérez, Hernández & Armstrong 2019). In contrast to the spatial data of mangroves and coral reefs, information on the distribution of seagrass beds is more difficult to obtain, especially in Indonesia (Dewi & Abidin 2021; Fauzan, Wicaksono & Hartono 2021). However, acquiring satellite imagery is now becoming easier with various medium-resolution images, for examples Landsat 8 and Sentinel 2A/2B provided by several international institutions such as NASA and ESA. Even though seagrass beds are objects below the water surface, their presence and distribution can still be observed (de Keukelaere et al. 2018; Gapper et al. 2018).

The classification technique, which is the analytical ability to distinguish seagrass from other shallow water objects such as coral reefs, sand, and coral fragments, is the main issue that limits the accuracy of seagrass identification using satellite imagery. Incorrect

classification techniques can have an effect on the resulting map and area calculations. The maximum likelihood algorithm is an example of pixel-based classification technique that produces excellent classification accuracy for high-resolution images such as World View 2 or Geo-Eye. However, several studies have shown a significant decrease in accuracy when using medium-resolution satellite imagery (Coffer et al. 2020; Kohlus et al. 2021; Lizcano-Sandoval et al. 2022). In recent years, there has been growing interest in using satellite images to map coastal ecosystems in significant details. Due to the access to medium-resolution satellite images is becoming widely available, it is critical to develop a proper classification method for mapping shallow water ecosystems such as seagrass beds.

The first objective of this study was to map the distribution of seagrass beds in Tanjung Benoa, Bali, using medium-resolution imagery, specifically Sentinel-2B. Second, in order to achieve more precise classification results, this study compares two classification methods: pixel-based image classification and object-based image classification. Pixel-based classification is performed for each land cover object using the supervised maximum likelihood classification method, which is guided by pixel values classified as objects through sample training (Hidayah & Wiyanto 2017). Meanwhile, object-based classification is used to define object classes based on spectral and spatial aspects simultaneously using multiscale segmentation (Hossain & Chen 2019).

The environmental quality of coastal areas with extensive human activity should be monitored on a regular basis. Tanjung Benoa is one of Bali's most popular tourist destinations for watersports. However, what is not yet clearly observed is the the state of its benthic ecosystem. Mapping the distribution and condition of seagrass beds is critical given the importance of its environmental function as well as other vital coastal ecosystems such as mangroves and coral reefs.

Materials and Methods

RESEARCH LOCATION AND TIME

This study was conducted at the Tanjung Benoa waters, located in Denpasar City, Bali, Indonesia (Figure 1). This location is well known as a centre for water sports and marine tourism in Bali. Tanjung Benoa is about 173.75 ha with an average depth of 5-6 m and characterized with calm waves. Some diving and snorkeling spots in this location are crowded with tourists, especially during the holiday season. Field data collection was carried out in October-December 2021. Retrieval of field data included identification of species and measurement of seagrass cover using quadratic transects. Data processing and analysis of satellite images were performed at the Center for Environmental Research of Udayana University.

SATELLITE IMAGE

Information on the benthic substrate was obtained by analyzing the Sentinel 2B Level 1C satellite image acquired on 23 November 2021. The Sentinel 2B satellite was launched in March 2017, preceded by the Sentinel 2A satellite launch in June 2015. These two satellites have the same characteristics. Therefore, they are often called twin satellites. The Sentinel-2 satellite carries onboard multispectral imaging (MSI) instrument with the capability to record 13 bands of the wave spectrum at a wavelength of 0.433-2190 µm (Table 1). Sentinel 2A and 2B images can be accessed freely through the Copernicus Open Access Hub (https://scihub.copernicus.eu/). The wave spectrum channel used was bands 2, 3 and 4 (blue, green and red) with 10 m × 10 m spatial resolution.

FIELD DATA COLLECTION AND ANALYSIS

Field data collection was carried out using the UPT (Underwater Photo Transect) method with a 10 m × 10 m transect adjusted to the resolution of the Sentinel-2B image. Photographs were taken nine times on each 10 m × 10 m transect and ground truth habitat using a 1 m × 1 m quadrant transect as the photo frame area (Figure 2). Furthermore, the field data collection survey of benthic habitats used the purposive sampling method, which considered the diversity of shallow marine bottom habitat classes.

Data processing was conducted by organizing each field data in coordinate points and classification classes according to objects. The field data used were 195 sample points in the form of a 10 m × 10 m transect (Figure 3). The data for the classification and accuracy test consisted of the coordinates of each class with a ratio of 1:1 in each class. The Quantum GIS software converted the classification and accuracy test results into .shp file format. This format change simplifies the classification process and tests accuracy when processing image data.
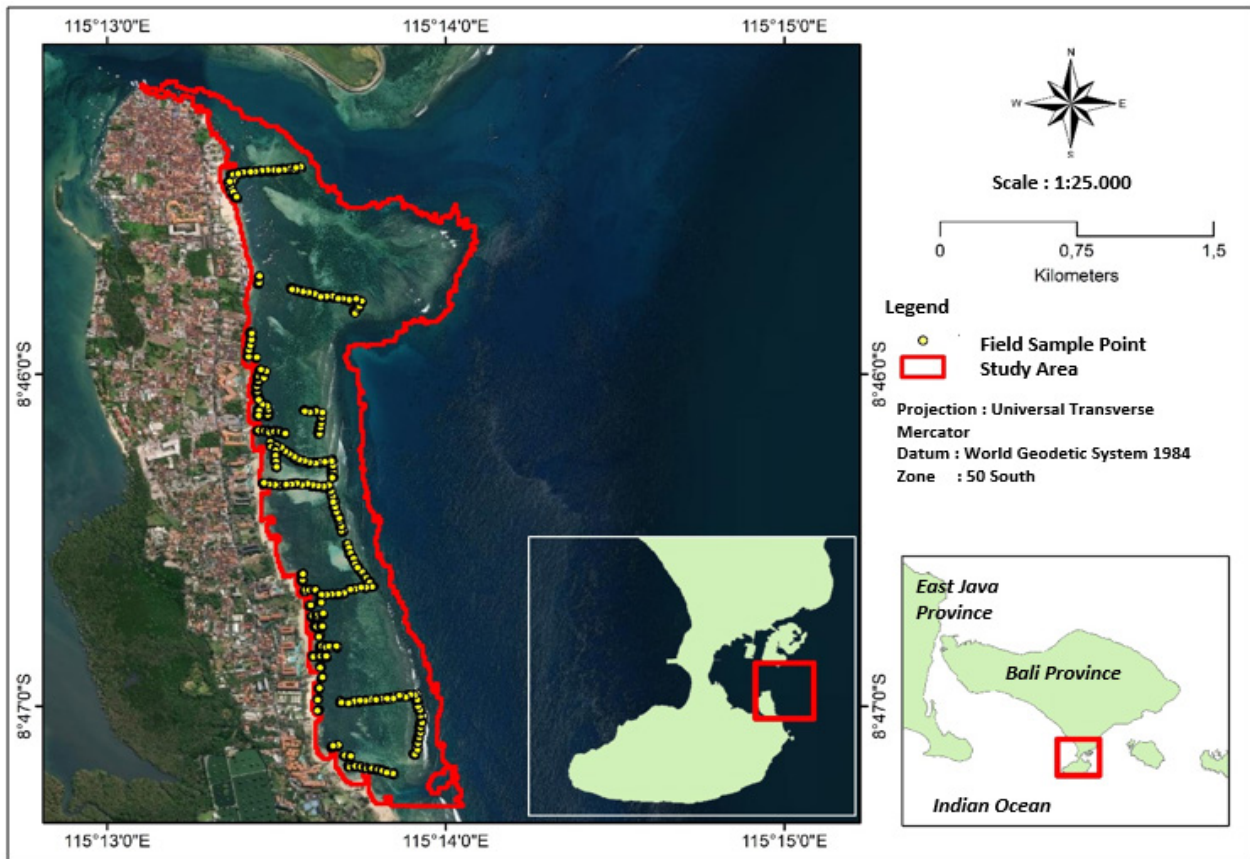
FIGURE 1. Research location showing the area of Tanjung Benoa and
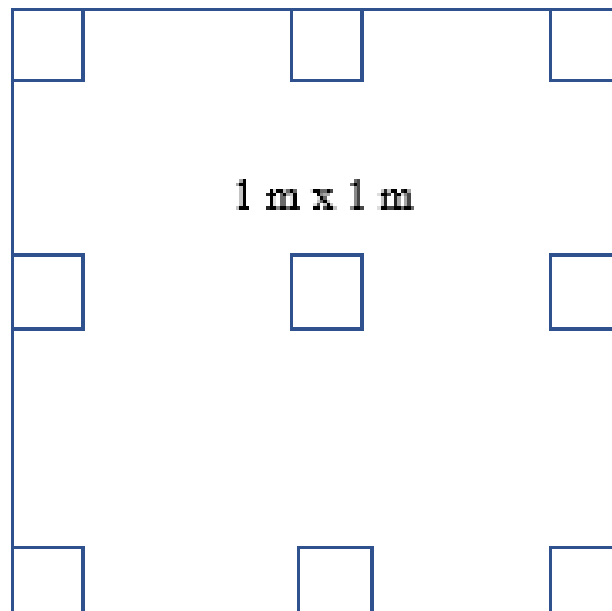seagrass field sampling points

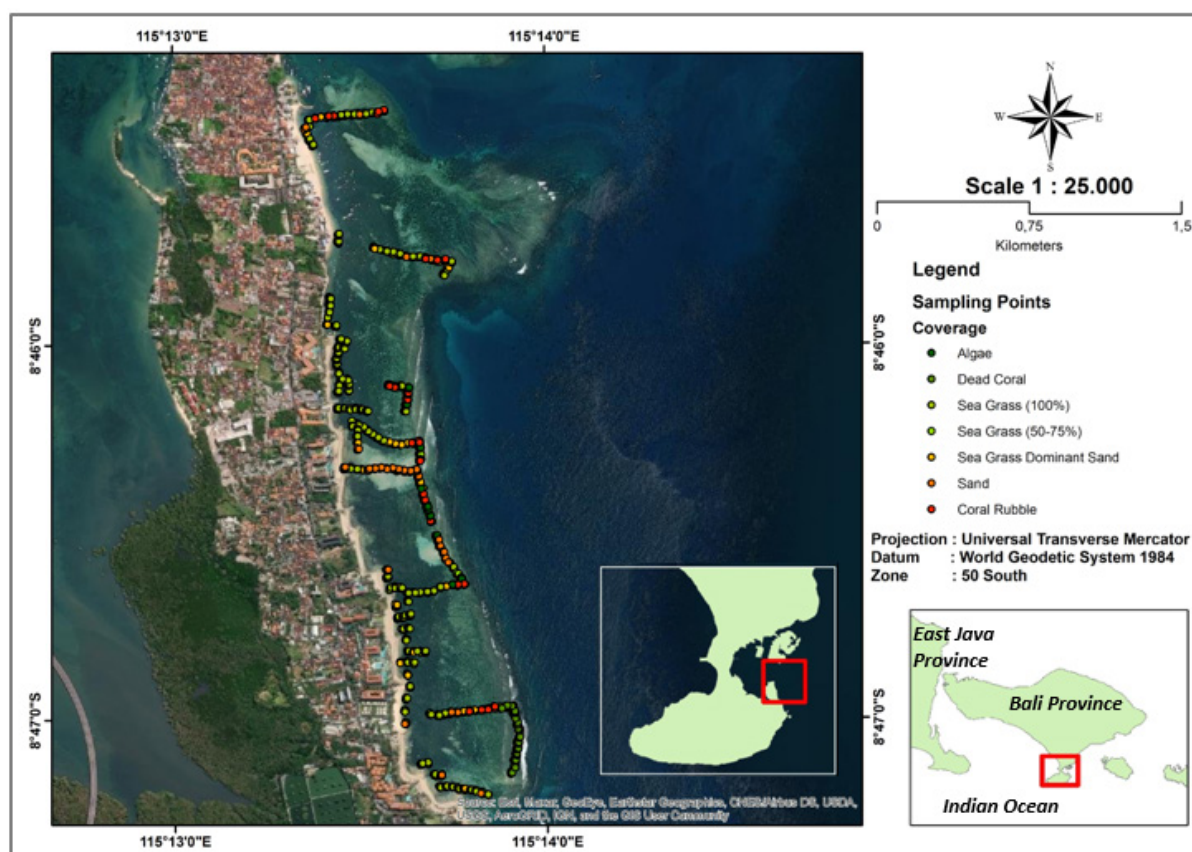FIGURE 2. 10 m × 10 m transect for field data collection

FIGURE 3. Classification of 10 m × 10 m sample points by cover class

TABLE 1. Basic characteristics of Sentinel 2B multi-spectral instruments

Band	Resolution	Wavelength (μm)	Description
B1	60	0,433	Ultra-Blue coastal and aerosol
B2	10	0,490	Blue
B3	10	0,560	Green
B4	10	0,665	Red
B5	20	0,705	Visible and Near Infrared (VNIR)- vegetation red edge 1
B6	20	0,740	Visible and Near Infrared (VNIR)- vegetation red edge 2
B7	20	0,783	Visible and Near Infrared (VNIR)- vegetation red edge 3
B8	10	0,842	Near-Infrared (NIR)
B8A	20	0,865	Narrow Near Infrared (NNIR)
B9	60	0,945	Short Wave Infrared (SWIR) - water vapour
B10	60	1,375	Short Wave Infrared (SWIR)- cirrus
B11	20	1,610	SWIR
B12	20	2,190	SWIR

SATELLITE IMAGE PROCESSING

Sentinel-2B Level 1C image pre-processing includes radiometric correction, stacking, cropping, and masking. The radiometric correction made is the Bottom of Atmosphere (BOA) correction. The BOA correction process was conducted using the Dark Object Subtraction (DOS) method available on the Semi-Automatic Classification Plugin (SCP) tool in the Quantum GIS software. This plugin provides a set of interrelated analysis tools and a user interface to simplify and automate the land cover classification phase, from downloading to processing satellite imagery (Congedo 2021).

The results of the pre-processing of the Sentinel-2B image were then continued with water column correction using Depth Invariant Index (DII). Water column correction improves image quality by eliminating disturbances using the Lyzenga algorithm. The correction assumes that the light entering the water column will decrease exponentially with increasing depth (attenuation). Furthermore, the correction uses visible light band composition by extracting the spectral value of the image on the substrate type from different depths. The pair of bands used is band 2 (blue), band 3 (green), and band 4 (red), and the Lyzenga algorithm formulation is as follows:

$$\text{Depht Invariant Index} =$$

$$\text{Ln (Li)} - \left[\left(\frac{ki}{kj}\right)\text{xLn (Lj)}\right]\frac{ki}{kj} = \sqrt{(a + (a^2 + 1))}$$

$$a = \frac{(\text{var Li} - \text{var Lj})}{(2 \text{ x cov Li. Lj})}$$

where Li is the spectral value of the green channel on the Sentinel 2B image; and LJ is the spectral value of the blue channel on the Sentinel 2B image.

The object-based classification method or OBIA (Object-Based Image Analysis) is conducted by segmenting the image using the MRS (Multi-Resolution Segmentation) algorithm. Segmentation with this algorithm is based on three parameters, namely scale, shape, and compactness. These three parameters will be used as input features to build a rule set in the process tree. The rule is a collection of several algorithms used to classify objects into certain classes. The MRS algorithm has the following equation:

$$S_f = w_{colour} \text{ x } h_{colour} + (1 - w_{colour}) \text{ x } h_{shape}$$

where S_f is the segmentation function; w_{colour} is the colour parameter weight; h_{colour} is the colour parameters; h_{shape} is the shape parameter weight; and w_{colour} is the shape parameter.

The multiscale classification concept developed consists of two levels of image objects, specifically level 1 (reef level) and level 2 (benthic habitat). Classification at level 1 applies a threshold value to produce the desired object. The threshold value is obtained from try and error to determine the optimum value, and at level 1, the segmentation uses a scale of 10. Classes at level 1 consist of land with shallow and deep water separated using a threshold value of NDVI (Normalized Difference Vegetations Index) by dividing the difference of pixel value in the Near Infrared (NIR) band and Red band by the sum of NIR and Red band. Negative values of NDVI (values approaching -1) correspond to water while valus close to zero (-0.1 to 0.1) generally correspond to sand or land. Shallow water segmentation at level 2 uses a scale of 5, and the classification uses a classifier by applying the Support Vector Machine (SVM) algorithm with a thematic layer for benthic habitat classes. The SVM algorithm is as follow (Tzotsos 2006):

$$f(x): \sum \zeta i y_i K(x_i x) + w_0$$

where K is the kernel function; x_i is the training sample; ζ_i is the lagrange; S is the part of the training sample corresponding to the non-zero lagrange multiplier; and w_0 is the hyperplane parameters.

Pixel value-based classification was conducted with a guided classification using the Maximum Likelihood algorithm. Maximum Likelihood classification considers the maximum probability of several pixels in the input image. This method aims to minimize class overlap. This method uses Region of Interest (ROI) data as a classification reference in field data. The algorithm used is based on the Bayesian equation as follow:

$$P = \ln(A_c) - 0,5\ln(|\Sigma_c|) - 0,5[(x - \mu c)^T(\Sigma_c^{-1})(X - \mu c)]$$

where P is the likelihood distance weight; C is the class index; X is the pixel value of candidate class; μc is the average of training for class c; A_c is the priori percentage for class c; $|\Sigma_c|$ is the determinant of the variance matrix for class c; Σ_c^{-1} is the inverse diversification matrix for class c; and T is the matrix round.

The classification results of remote sensing data were validated using an error matrix (confusion matrix). This method compares image classification results with the observations in the field (Kovacs et al. 2018; León-Pérez, Hernández & Armstrong 2019). The accuracy test consisted of overall accuracy (OA), producer (PA), and user accuracy (UA). The OA value is correctly the overall percentage of classed pixels, the PA value is the average probability of a pixel showing the distribution of each class in the field (Poursanidis et al. 2019), and the UA is the average probability of a pixel representing a particular class. The calculation of the accuracy value was based on the following equations:

$$\text{Overall accuracy} = \frac{\sum_{i=1}^{k} n_{ii}}{n}$$

$$\text{Producer accuracy} = \frac{n_{jj}}{n+j}$$

$$\text{User accuracy} = \frac{n_{ii}}{n_{i+}}$$

After calculating the accuracy value, the kappa value of each error matrix in each experiment was calculated. The Kappa test is used to assess the accuracy of the error matrix (Richards & Jia 2006), and the coefficient has a range of 0-1 (Table 2) and is calculated by the following equation:

$$\text{Kappa coefficient (K)} = \frac{N \sum_{i=1}^{r} x_{ii} - \sum_{i=1}^{r}(x_{i+}, x_{+i})}{N^2 - \sum_{i=1}^{r}(x_{i+}, x_{+i})}$$

where r is the number of rows in matrix; x_{ii} is the number of observations in row i and column i; x_{i+} and x_{+i} is the Marginal total of row i and column i, respectively; N is the total observations.

RESULTS AND DISCUSSION

SEAGRASS COVER

Seagrass bed communities in the shallow waters of Tanjung Benoa can be found at a distance of 0-400 m from the shoreline (Figure 3). Analysis of seagrass cover in benthic environments showed mixed results. Table 3 summarizes 195 transects with 1,746 sample points. Seagrass cover of 75%-100% appears to dominate, with the percentage reaching 40.78% of the total sample points. Furthermore, 15.41% and 17.98% points obtained results from 50% and 25% seagrass cover, while around 25% of the sample points obtained results without seagrass cover (Table 4).

TABLE 2. Kappa coefficient alue range for accuracy test

Kappa coefficient value	Classification
<0.4	Bad accuracy
0.41–0.60	Medium accuracy
0.61–0.80	Good accuracy
>0.80	Excellent accuracy

TABLE 3. Field observation results of seagrass cover

Seagrass cover (%)	Number of points	Percentage (%)
0	451	25.83
25	314	17.98
50	269	15.41
75	347	29.87
100	365	10.90
Total	195	100

TABLE 4. Observations of 1 m × 1 m transect cover class

Cover class	Number of points	Percentage (%)
Algae	52	2.98
Dead coral	112	6.99
Seagrass (<50%) sand dominant	17	0.50
Seagrass 75%	721	41.29
Seagrass 100%	568	32.53
Sand	174	9.97
Coral fragments	102	5.84
Total	195	100

BOA CORRECTION

The atmosphere affects the travel of electromagnetic waves from the sun to the object and from the object to the sensor, which causes a difference in the reflectance value of the image. This atmospheric effect (noise) is divided into molecular (rayleigh scattering) and particle (noodle scattering or aerosol scattering) effects. Therefore, atmospheric correction is needed to eliminate these effects on remote sensing data recorded by satellite sensors. The reflectance value in the analysis of satellite imagery was divided into Top of Atmosphere (TOA) reflectance captured by the sensor while BOA reflectance was corrected by the atmosphere. Sentinel 2B image used is Level 1C which has undergone geometric and TOA correction. This is effective for correcting atmospheric disturbances such as the effect of water vapor and aerosol in the form of thin fog, smoke, and thin clouds (Ariza, Robredo Irizar & Bayer 2018; de Keukelaere et al. 2018). The BOA correction results can change the digital value of image pixels into reflectance values received by objects (Table 5).

WATER COLUMN CORRECTION

Water column correction was carried out by calculating the Depth Invariant Index (DII), which used information from the ratio of the attenuation coefficient for each pair of visible light bands (K_i/K_j) (Table 6). Then, the best band pair selection was carried out based on the regression parameter of the logarithmic value of the pixel values in each band (Gapper et al. 2018). The regression relationship for each pair is presented in Figure 4, and the results show that the pairs of bands 2 and 3 (blue and green) had better results than others with $R^2 = 0.9594$.

The algorithm was then transformed into image data to correct the water column. The results were used to classify benthic habitats and seagrass beds. The difference between corrected and uncorrected data was obvious since there was a visible color shift on the sand substrate in the waterways. They seemed brighter and clearer than those without adjusted water columns. Conversely, the uncorrected image of the sand substrate water column looks bluish (Figure 5).

MULTISCALE OBJECT-BASED IMAGE CLASSIFICATION

The basic of the object-based image classification (OBIA) process is segmentation (Ariza, Robredo Irizar & Bayer 2018; Dattola et al. 2018). Classification level 1 (reef level) aims to classify land areas, shallow waters, and deep waters (Figure 6). This process uses the threshold value (threshold) of NDVI (Normalized Difference Vegetation Index). The value for the land, shallow water, and deep water are 0.0345 and 0.345. There are 283.87 ha of land, 288.59 ha of shallow water, and 551.64 ha in the entire study area based on categorization findings from level 1.

After obtaining shallow water classes at level 1, re-segmentation was conducted for classification at level 2. The results of level 1 classification were used for

level 2 where shallow water areas were classified into two thematic layers, consisting of six benthic habitats with seagrass and non-seagrass classes. This advanced and multi-stage classification aims to improve pixel segmentation in various classes.

Level 2 classification was conducted by a guided classification method using the Support Vector Machine (SVM) algorithm with the layer values (mean and standard deviation) of all visible light bands and the composition of DII band pairs. The results of level 2 classification in six benthic habitats with seagrass and non-seagrass classes are presented in Figure 7. Classification level 2 in six benthic habitat classes obtained the area of each class, including seagrass class of 242.99 ha, seagrass and sand of 4.92 ha, death coral of 2.47 ha, algae of 0.19 ha, ruble of 6.05 ha, and sand of 2.23 ha from a total area of 258.85 ha. The level 2 classification for seagrass and non-seagrass classes obtained an area of 246.60 ha for the seagrass and 12.25 ha for the non-seagrass class.

TABLE 5. Sentinel-2B image pixel values corrected for BOA

Band	Pixel value before BOA correction				Pixel value after BOA correction			
	Min	Max	Mean	Stdev	Min	Max	Mean	Stdev
Band 2	346	15,493	1,615.435	1,698.148	0	10,000	958.5119	1,686.887
Band 3	1	14,977	1,326.535	1,746.349	0	10,000	924.2323	1,733.284
Band 4	1	16,598	1,142.855	1,907.661	0	10,000	968.2271	1,877.899

TABLE 6. Calculation of the Lyzenga algorithm

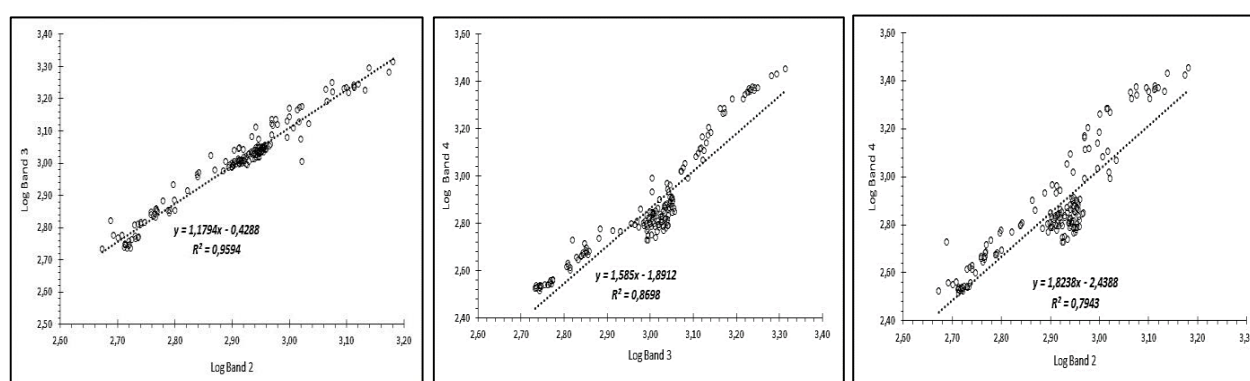| Band	Band	Covariance	A	Ki/Kj	Algorithm
Band 2	B2/B3	0,014423	-0,191838	0,82639	alog(b2)-(0.8264*(alog(b3)))
Band 3	B2/B4	0,022304	-0,879035	0,45239	alog(b2)-(0.45239*(alog(b4)))
Band 4	B3/B4	0,028102	-0,599216	0,56657	alog(b3)-(0.56657*(alog(b4)))

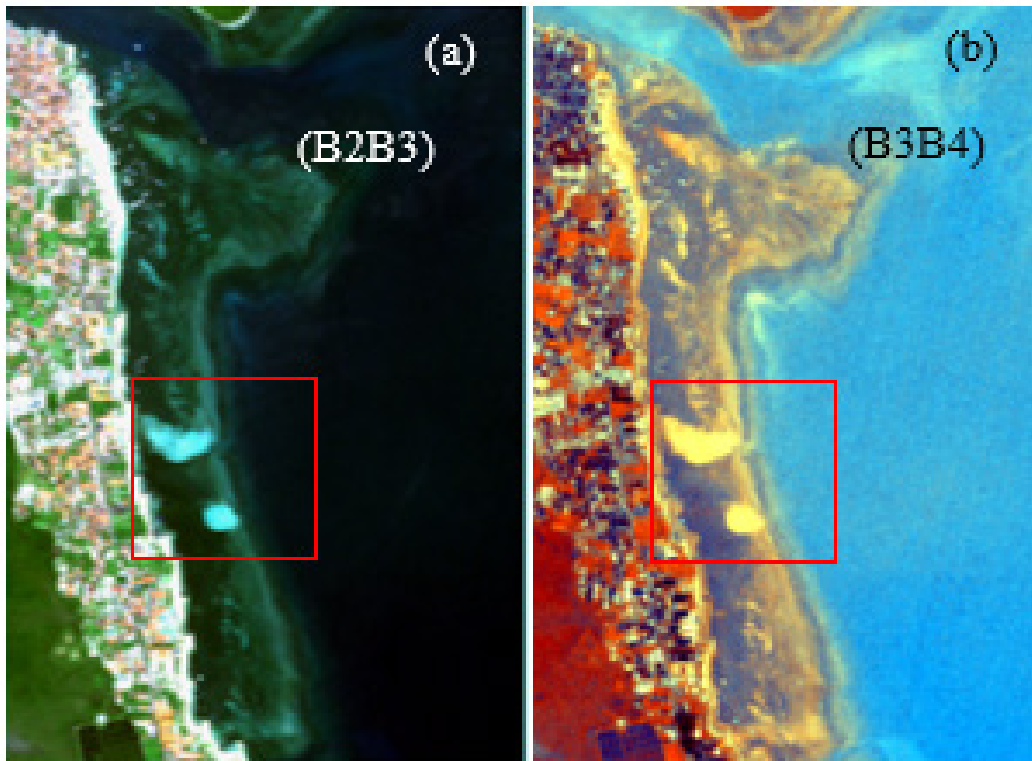FIGURE 4. Regression analysis of band pairs 2,3 and 4 on Sentinel Image 2B

FIGURE 5. Image of Sentinel-2B (a) before water column correction and (b) after water column correction
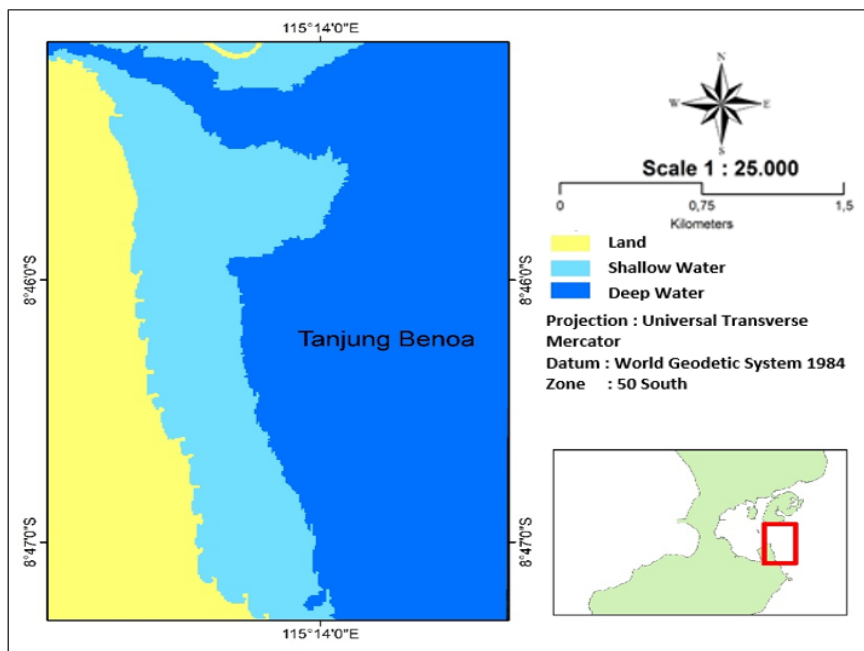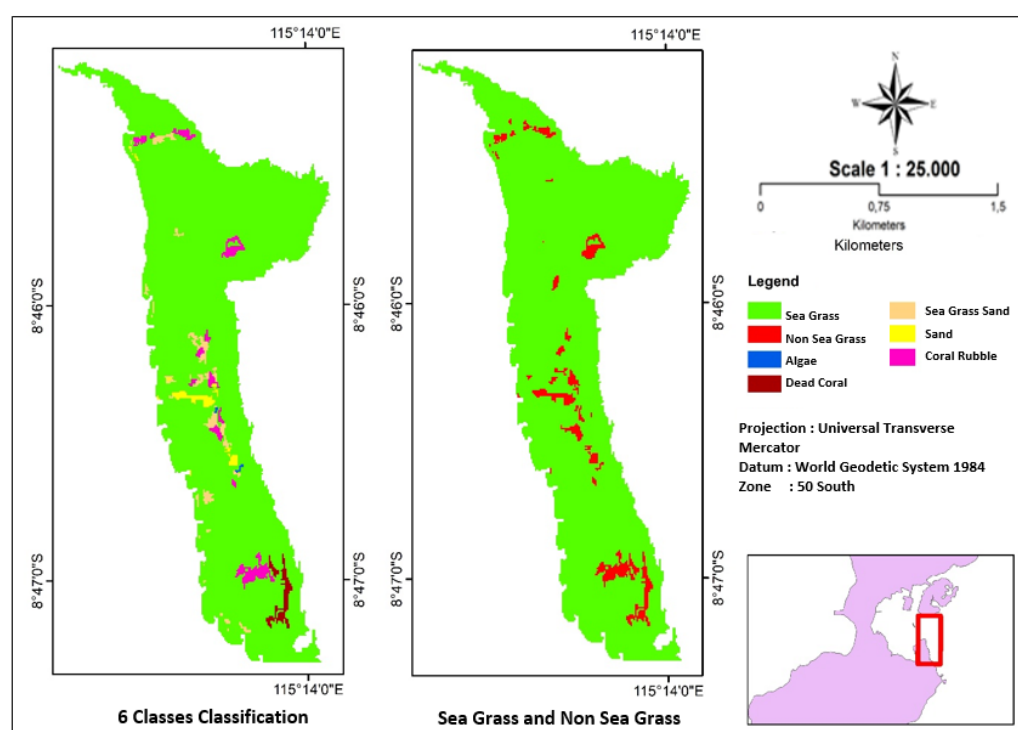

FIGURE 6. Level 1 classification

FIGURE 7. Object-based level 2 classification with SVM algorithm

CLASSIFICATION BASED ON PIXELS/MULTISPECTRAL

Pixels/Multispectral was used for the classification of six benthic habitats with seagrass and non-seagrass classes by cutting the combined DII band according to the shallow water area due to level 1 classification in the OBIA method. The combined DII band image was classified using the Maximum Likelihood algorithm through the ROI of field data. The maximum Likelihood algorithm is commonly used in supervised classification techniques with remote sensing satellite imagery data or other underwater vehicles to identify types of shallow bottom substrate cover (Hidayah & Wiyanto 2017; Kovacs et al. 2018; Mogstad, Johnsen & Ludvigsen 2019; Niroumand-Jadidi, Pahlevan & Vitti 2019; Poursanidis et al. 2021). The algorithm groups the unknown pixels based on the average vector and the variance matrix of each information class spectral pattern. Image pixels are entered into one class with the highest probability (opportunity). This Maximum Likelihood classification evaluates the variance and covariance of the category spectral response patterns quantitatively when classifying unknown pixels. The classification results of the six benthic habitats with the seagrass and non-seagrass classes are shown in Figure 8.

The results of level 2 classification of six benthic habitats and seagrass and non-seagrass classes with different methods and algorithms gave different distribution and classification results. However, this study used the same field data for classification in each method (Table 7). The wide difference was caused by the way the pixel values were read and the grouping of each pixel into the desired classification class by each method and algorithm.

ACCURACY TEST

The difference in the results of level 2 classification in the object-based and pixel-based methods showed differences in the process and execution of each method in classifying benthic habitats. Additionally, the different results of this classification method gave different distribution and area results. Therefore, the best classification results were achieved by performing an accuracy test on each classification. The accuracy test on the classification of six benthic habitats with seagrass and non-seagrass classes used 872 field data consisting of all classification classes. The confusion matrix results are presented in Table 8 and were used to determine the accuracy of the classification findings in this study.
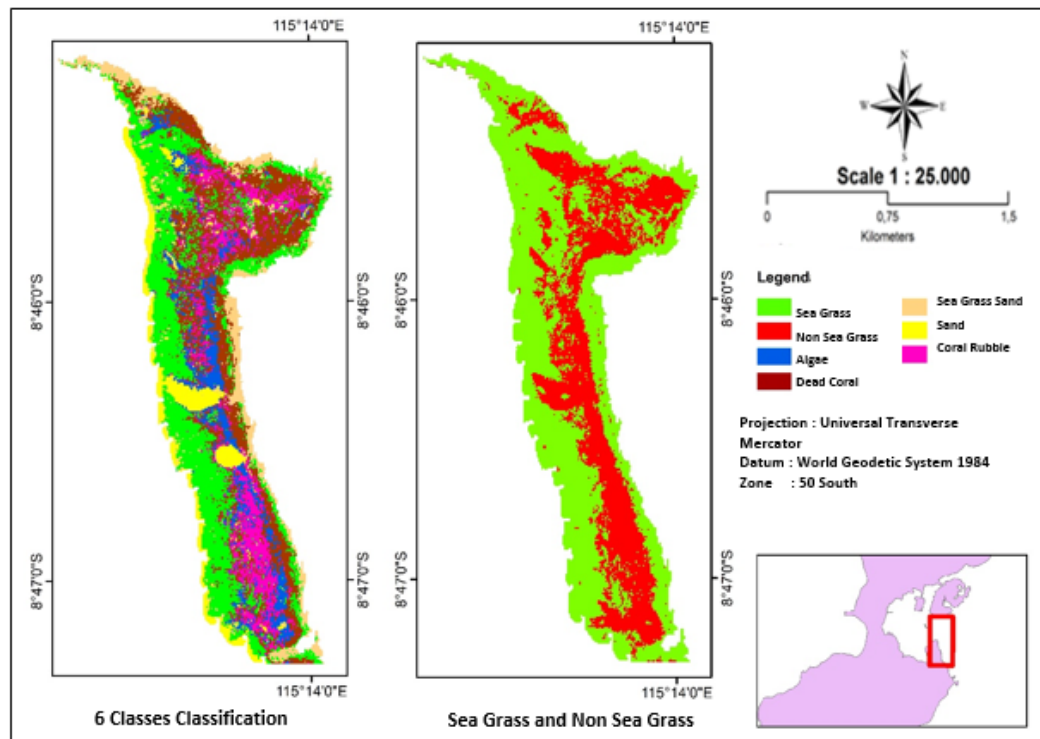
FIGURE 8. Pixel-based level 2 classification with Maximum Likelihood algorithm

The accuracy test on the classification results showed that the number affects the accuracy level. This is evident from the overall accuracy value in the classification of two classes greater than the six classes classification of benthic habitats. The overall accuracy value of the object-based SVM algorithm classification with two classes was 85.43%, and for the six classes was 77.71%. Meanwhile, the overall accuracy value of the pixel-based Maximum Likelihood algorithm classification with two classes was 71.01%, and six classes of benthic habitat were 50.62%. Based on this accuracy test, the classification method with the best value was the OBIA-based classification method with the SVM algorithm. The two classes of seagrass and non-seagrass with the six benthic habitat classes were included. A higher level of object-based classification accuracy than pixel-based was found in other seagrass research and mapping, such as in the Thousand Islands

north of Jakarta and Kodingareng Lompo Island, Spermonde Islands in southwest Sulawesi (Sabilah, Siregar & Amran 2021; Siregar et al. 2018).

Based on the results of object-based classification, the optimistic estimate of the area of the seagrass community in Tanjung Benoa is around 242.99 ha, with an average dominant cover of 75%. Seven species of seagrass were found, namely *Cymodocea serrulata, Cymodocea rotundata, Thalassia hemprichii, Syringodium isoetifolium, Halodule pinifolia, Halodule ovalis,* and *Halodule uniervis.* Previously published research data found a higher composition of seagrass in the Riau Islands with ten species (Kawaroe et al. 2016). Meanwhile, research conducted on Liki Island and Meossu Island in Papua succeeded in making an inventory of seven seagrass species. The summary of the percentage of seagrass cover and species from the 2016-2021 research is presented in Table 9.

TABLE 7. Class area (ha) of benthic habitat based on image classification result

Classification Method	Six Classes						Two Classes		Area
	Seagrass	Seagrass and sand	Algae	Dead coral	Sand	Ruble	Seagrass	Non-seagrass	
OBIA-SVM	242.99	4.92	0.19	2.47	2.23	6.05	246.6	12.25	258.85
Pixels-Maximum Likelihood	82.35	27.32	24.81	68.19	22.26	33.98	161.18	97.73	258.91

TABLE 8. Classification accuracy test results

| Classification | OBIA-based | | | | Pixel-based | | | |
| | SVM algorithm | | | | Maximum likelihood algorithm | | | |
	Kappa	OA (%)	PA (%)	UA (%)	Kappa	OA (%)	PA (%)	UA (%)
Six Classes	**0.6506**	**77.7019**			**0.3355**	**50.625**		
Seagrass			85.89	85.37			60	9.28
Seagrass and sand			61.87	61.87			63.41	31.71
Algae			44.44	21.05			62.87	84.31
Dead coral			96.77	98.36			1.67	16.67
Sand			90.36	83.33			78.46	54.84
Rubles			39.18	61.29			36.84	20.79
Two Class	**0.6202**	**85.4358**			**0.3823**	**71.0069**		
Seagrass			89.7	90.39			69.4	87.8
Non-seagrass			72.32	71.37			75.16	48.79

OA = Overall Accuracy, PA = Producer Accuracy, UA = User Accuracy

Even though the seagrass community condition in Tanjung Benoa is relatively better, several factors need to be considered to prevent it from serious environmental damage. The sustainability of seagrass communities is highly dependent on the physical and chemical conditions of the waters. The main cause of damage to seagrass communities is the decreased water clarity due to high water turbidity or the entry of nutrients into the waters. The increase in the concentration of dissolved solids in the waters is caused by deforestation in the upstream part of the river and the cutting of mangroves in the coastal area (Sjafrie et al. 2018; Unsworth et al. 2018). Furthermore, pollution due to industry and aquaculture causes the waters to be exposed to excessive nutrients (Hasan & Widodo 2020; Nurjirana et al. 2022; Pardamean et al. 2021). These variables may obstruct the photosynthetic process of seagrass, posing a barrier to development. Human activities that contribute to the decline in seagrass areas include beach reclamation, dredging, and sand mining, as well as oil pollution (Kawaroe et al. 2016; Unsworth et al. 2018). Pollution from oil spills can kill marine mammals, seaweed, coral reefs, and fish, leading to an imbalance in the food web (Gani et al. 2015; Hasan & Islam 2021; Hasan et al. 2021). It can also damage habitats and breeding grounds for marine animals. In the event of an oil leak, the effects might last for decades (Davies et al. 2014). Uncontrolled tourism activities can also threaten seagrass conditions. Seagrass beds can be damaged if repeatedly stepped on by tourists. The heavy tourist boat traffic can also directly disturb the marine life in the seagrass beds. Therefore, it is necessary to have a clear zoning division of the tourist area by prioritizing the protection area for seagrass ecosystems and marine biota in it.

TABLE 9. Percentage of seagrass cover and distribution of seagrass species in Indonesia

Location	Estimated coverage	Seagrass species										Source
		Cr	Cs	Ea	Hm	Ho	Hs	Hp	Hu	Si	Th	
Spermonde Islands	50%	+	-	+	-	-	-	-	+	+	+	Thalib, Nurdin & Aris (2018)
Riau Islands	61%	+	+	+	+	+	+	+	+	+	+	Kawaroe et al. (2016)
Seribu Islands	37%	+	+	+	-	-	-	-	+	+	+	Kawaroe et al. (2016)
Talaud Islands	43%	+	-	-	-	-	+	-	+	+	+	Kawaroe et al. (2016)
Lobam Island	30%	-	-	+	-	-	-	-	-	-	+	Prarikeslan et al. (2019)
Tanimbar Island	60%	+	-	+	+	+	-	-	+	+	+	Kawaroe et al. (2016)
Lombok Island	30%	+	-	+	+	-	-	-	+	-	+	Rahman, Qayim & Wardiatno (2018)
Tayando Island	43%	+	+	+	-	+	-	+	-	+	+	Fitrian, Kusnadi & Persilette (2017)
Bunaken Island	30%	+	-	+	-	-	-	+	-	+	+	William-Schaduw & Ivone Kondoy (2020)
Siladen Island	29%	+	-	+	-	-	-	+	-	+	+	William-Schaduw & Ivone Kondoy (2020)
Manado Tua Island	19%	-	-	-	-	-	-	+	+	+	+	William-Schaduw & Ivone Kondoy (2020)
Mantege Island	33%	+	-	-	-	-	-	+	-	-	+	William-Schaduw & Ivone Kondoy (2020)
Nain Island	26%	+	-	+	-	-	-	-	-	-	-	William-Schaduw & Ivone Kondoy (2020)
Liki Island	82%	+	-	+	-	+	-	+	+	+	+	Nugraha et al. (2021)
Meossu Island	62%	+	-	+	-	+	-	+	+	-	+	Nugraha et al. (2021)
Befondi Island	31%	+	-	-	-	-	-	-	-	-	+	Nugraha et al. (2021)

Description: + (present), and - (absent).

Seagrass species: Cr = *Cymodocea rotundata*, Cs=*Cymodocea serrulata*, Ea=*Enhalus acoroides*, Hm=*Halophila minor*, Ho=*Halophila ovalis*, Hs= *Halophila spinulosa*, Hp=*Halodule pinifolia*, Hu= *Halodule uninervis*, Si=*Syringodium isoetifolium*, and Th= *Thalassia hemprichii*

As a typical coastal ecosystem that is susceptible to harm from natural and human influences, spatial data monitoring of the environment is critical. Lack of detailed spatial information on coastal resources, especially mangroves, seagrasses, and coral reefs, hinders efforts for protection and management in the face of global climate change and anthropogenic impacts (Islamy & Hasan 2020; Poursanidis et al. 2019). The utilization of satellite imagery is useful for routinely generating spatial data on land and coastal environments with large areas (Adebayo, Otun & Daniel 2019; Dangulla, Munaf & Mohammad 2020; Fauzan, Wicaksono & Hartono 2021). However, since access to high-resolution satellite pictures is restricted, medium-resolution satellite images such as Sentinel 2 and Landsat 8 accessed freely may serve as the primary alternative source of spatial data for environmental monitoring operations. This study showed that Sentinel-2 imagery can be used well for seagrass mapping because of the good spatial resolution, band availability, and radiometric accuracy.

Due to the difference in spatial resolution, the accuracy factor needs to be considered for more detailed mapping, especially for seagrass beds. The overall accuracy generated from high-resolution images such as World View 2 (1.85 meters spatial resolution) or MIVIS (3 meters spatial resolution) is higher than Sentinel 2 or Landsat 8 images (Dattola et al. 2018), even though the resulting accuracy reaches more than 90% (Coffer et al. 2020; Ha et al. 2020; León-Pérez, Hernández & Armstrong 2019). In coastal places, the pixel reflection value might be affected by the occurrence of tides, even when utilizing high-resolution photos. An increase in the water volume above the shallow bottom at high tide will increase satellites' attenuation and spectral absorption (Kovacs et al. 2018).

The image classification comparison in this study confirms that the multiscale object-based classification method with the SVM algorithm has better results than the pixel-based with the maximum likelihood algorithm. The application of multiscale classification separates seagrasses from other underwater objects, therefore, the classification results are more accurate (Rahman 2013). Research in Tauranga Harbor, New Zealand showed that the classification using the maximum likelihood algorithm fails to distinguish rare seagrass cover from the sand substrate, and hence intervention through machine learning approaches is needed to produce a better classification (Ha et al. 2020). Combining high-resolution satellite imagery and OBIA with the SVM or Fuzzy Logic algorithm can provide excellent results for classifying seagrasses based on their cover density (Sabilah, Siregar & Amran 2021).

Besides, utilizing multispectral satellite imagery due to remote sensing technology with a spacecraft platform, mapping shallow bottom substrate cover can be conducted with several other techniques. Underwater Hyper-Spectral Imaging through an Unmanned Surface Vehicle has been tested for mapping the bottom substrate of the waters in Trondheim, Norway (Mogstad, Johnsen & Ludvigsen 2019). This approach can map six seabed cover types with an accuracy rate of 89%-91% using photos with a spatial resolution of 0.5 cm. Even though the total accuracy produced by this technique is quite high, specific results have not been obtained for seagrass beds. Meanwhile, another technique for mapping seagrass beds uses the hydro-acoustic method (Manik & Apdillah 2020). The quantity of seagrass biomass may be calculated using back-scattering strength value analysis. The accuracy value obtained for the classification of bottom substrate cover was quite high, reaching 87%. USV or hydro-acoustic equipment mounted on the research ships can be an alternative for mapping seagrass beds for small water areas, while satellite imagery is more of an option for larger water areas.

In addition, SVM produces significantly good results for linearly separable data. The SVM algorithm divides hyperplanes to maximize the margin of separation between classes measured along a line perpendicular to the hyperplane. In SVM, a hyperplane is a decision boundary that separates the two classes, where a data point on either side of the hyperplane can belong to distinct classes. As a result, the algorithm will select the best line that separates the data as well as maximize the distance between data points from different classes.

However, some limitations of using SVM for satellite image classification must be considered. Because SVM relies heavily on clear class boundaries, it will underperform when target classes overlap (Medina & Atehortua 2018). In comparison to other classification algorithms such as maximum likelihood or random forest, in order to avoid confusion in the classification of non-sampled areas, SVM requires a number of classes that comprehensively represent the variations of the image to guarantee a minimum number of support vectors.

CONCLUSION

This study has demonstrated the ability of Sentinel 2B imagery to detect the type of shallow bottom substrate cover in Tanjung Benoa Bali. This study discovered a number of seagrass species that are commonly found in

Indonesian waters. The area of mapped seagrass beds is estimated at 242.99 ha, with an average cover of 75%. Based on the comparison of different image classification approach, it is confirmed that the object-based image approach with SVM algorithm outperforms the pixel-based approach with the Maximum Likelihood algorithm in terms of classification accuracy.

REFERENCES

Adebayo, H.O., Otun, W.O. & Daniel, I.S. 2019. Change detection in land use/landcover of Abeokuta metropolitan area, Nigeria using multi-temporal Landsat remote sensing. *Indonesian Journal of Geography* 51(2): 217-223.

Ambo-Rappe, R., La Nafie, Y.A., Marimba, A.A. & Unsworth, R.K.F. 2021. Seagrass habitat characteristics of seahorses in Selayar Island South Sulawesi Indonesia. *AACL Bioflux* 14(1): 337-348.

Ariza, A., Robredo Irizar, M. & Bayer, S. 2018. Empirical line model for the atmospheric correction of sentinel-2A MSI images in the Caribbean Islands. *European Journal of Remote Sensing* 51(1): 765-776.

Brown, M.I., Pearce, T., Leon, J., Sidle, R. & Wilson, R. 2018. Using remote sensing and traditional ecological knowledge (TEK) to understand mangrove change on the Maroochy River, Queensland, Australia. *Applied Geography* 94(1): 71-83.

Coffer, M.M., Schaeffer, B.A., Zimmerman, R.C., Hill, V., Li, J., Islam, K.A. & Whitman, P.J. 2020. Performance across WorldView-2 and rapid eye for reproducible seagrass mapping. *Remote Sensing of Environment* 250(2): 37-49.

Congedo, L. 2021. Semi-automatic classification plugin: A python tool for the download and processing of remote sensing images in QGIS. *Journal of Open Source Software* 6(64): 3172-3182.

Cullen-Unsworth, L.C., Jones, B.L., Seary, R., Newman, R. & Unsworth, R.K.F. 2018. Reasons for seagrass optimism: Local ecological knowledge confirms presence of dugongs running. *Marine Pollution Bulletin* 134(1): 118-122.

Dangulla, M., Munaf, L.A. & Mohammad, F.R. 2020. Spatio-temporal analysis of land use/land cover dynamic in Sokoto metropolis using multi-temporal satellite data and land change modeller. *Indonesian Journal of Geography* 52(3): 306-316.

Dattola, L., Rende, F.S., Lanera, P., Di Mento, R., Dominici, R., Cappa, P., Scalise, S., Aramini, G. & Oranges, T. 2018. Comparison of Sentinel-2 and Landsat-8 OLI satellite images vs. high spatial resolution images (MIVIS and WorldView-2) for mapping *Posidonia oceanica* meadows. *Remote Sensing* 42(2). https://doi.org/10.1117/12.2326798. *SPIE*

Davies, T.W., Duffy, J.P., Bennie, J. & Gaston, K.J. 2014. The nature, extent, and ecological implications of marine light pollution. *Frontiers in Ecology and the Environment* 12(6): 347-355.

de Keukelaere, L., Sterckx, S., Adriaensen, S., Knaeps, E., Reusen, I., Giardino, C., Bresciani, M., Hunter, P., Neil, C., van der Zande, D. & Vaiciute, D. 2018. Atmospheric correction of Landsat-8/OLI and Sentinel-2/MSI data using iCOR algorithm: Validation for coastal and inland waters. *European Journal of Remote Sensing* 51(1): 525-542.

Dewi, A.N. & Abidin, Z. 2021. Analysis of the relationship of service quality, motivation and destination image to destination loyalty: a case study of Wonorejo mangrove ecotourism in Surabaya, East Java. *Journal of Aquaculture and Fish Health* 10(1): 46-55.

Fauzan, M.A., Wicaksono, P. & Hartono. 2021. Characterizing Derawan seagrass cover change with time-series Sentinel-2 images. *Regional Studies in Marine Science* 48(3): 1020-1048.

Fitrian, T., Kusnadi, A. & Persilette, R.N. 2017. Seagrass community structure of Tayando-Tam Island, southeast Moluccas, Indonesia. *Biodiversitas* 18(2): 788-794.

Fortes, M.D., Ooi, J.L.S., Tan, Y.M., Prathep, A., Bujang, J.S. & Yaakub, S.M. 2018. Seagrass in Southeast Asia: A review of status and knowledge gaps, and a road map for conservation. *Botanica Marina* 61(3): 269-288.

Gani, A., Nurjirana, Bakri, A.A., Adriany, D.T., Wuniarto, E., Khartiono, L.D., Satria, D.H., Hasan, V., Herjayanto, M., Burhanuddin, A.I., Moore, A.M. & Kobayashi, H. 2021. First record of *Stiphodon annieae* Keith & Hadiaty, 2015 (Teleostei, Oxudercidae) from Sulawesi Island, Indonesia. *Check List* 17(1): 261-267.

Gapper, J.J., El-Askary, H., Linstead, E. & Piechota, T. 2018. Evaluation of spatial generalization characteristics of a robust classifier as applied to coral reef habitats in remote islands of the Pacific Ocean. *Remote Sensing* 10(11): 105-125.

Ha, N.T., Manley-Harris, M., Pham, T.D. & Hawes, I. 2020. A comparative assessment of ensemble-based machine learning and maximum likelihood methods for mapping seagrass using sentinel-2 imagery in Tauranga Harbor, New Zealand. *Remote Sensing* 12(3): 1-16.

Hasan, V. & Widodo, M.S. 2020. The presence of Bull shark *Carcharhinus leucas* (Elasmobranchii: Carcharhinidae) in the fresh waters of Sumatra, Indonesia. *Biodiversitas* 21(9): 4433-4439.

Hasan, V. & Islam, I. 2021. First inland record of Bull shark *Carcharhinus leucas* (Müller & Henle, 1839) (Carcharhiniformes: Carcharhinidae) in Celebes, Indonesia. *Ecologica Montenegrina* 38: 12-17.

Hasan, V., Gausmann, P., Nafisyah, A.L., Isroni, W., Widodo, M.S., Islam, I. & Chaidir, R.R.A. 2021. First record of Longnose marbled whipray *Fluvitrygon oxyrhyncha* (Sauvage, 1878) (Myliobatiformes: Dasyatidae) in Malaysian waters. *Ecologica Montenegrina* 40: 75-79.

Hidayah, Z. & Wiyanto, D.B. 2017. Combining satellite image analysis and *in-situ* measurement to determine the condition of coral reef ecosystem of Mandangin Island, East Java, Indonesia. *Asian Journal of Microbiology, Biotechnology and Environmental Sciences* 19(3): 1-8.

Hidayah, Z., Rachman, H.A. & As-Syakur, A.R. 2022. Mapping of mangrove forest and carbon stock estimation of east coast Surabaya, Indonesia. *Biodiversitas* 23(9): 4826-4837.

Hossain, M.D. & Chen, D. 2019. Segmentation for Object-Based Image Analysis (OBIA): A review of algorithms and challenges from remote sensing perspective. *ISPRS Journal of Photogrammetry and Remote Sensing* 150(1): 115-134.

Islamy, R.A. & Hasan, V. 2020. Checklist of mangrove snails (Mollusca: Gastropoda) in south coast of Pamekasan, Madura Island, East Java, Indonesia. *Biodiversitas* 21: 3127-3134.

Kawaroe, M., Nugraha, A.H., Juraij & Tasabaramo, I.A. 2016. Seagrass biodiversity at three marine ecoregions of Indonesia: Sunda Shelf, Sulawesi Sea and Banda Sea. *Biodiversitas* 17(2): 585-591.

Kohlus, J., Stelzer, K., Müller, G. & Smollich, S. 2020. Mapping seagrass (Zostera) by remote sensing in the Schleswig-Holstein Wadden Sea. *Estuarine, Coastal and Shelf Science* 238: 106699.

Kovacs, E., Roelfsema, C., Lyons, M., Zhao, S. & Phinn, S. 2018. Seagrass habitat mapping: How do landsat 8 OLI, Sentinel-2, ZY-3A and Worldview-3 perform? *Remote Sensing Letters* 9(7): 686-695.

Lizcano-Sandoval, L., Anastasiou, C., Montes, E., Raulerson, G., Sherwood, E. & Muller-Karger, F.E. 2022. Seagrass distribution, areal cover, and changes (1990-2021) in coastal waters off west-central Florida, USA. *Estuarine Coastal and Shelf Science* 279(1): 108-134.

León-Pérez, M.C., Hernández, W.J. & Armstrong, R.A. 2019. Characterization and distribution of seagrass habitats in a Caribbean Nature Reserve using high-resolution satellite imagery and field sampling. *Journal of Coastal Research* 35(5): 937-947.

Manik, H.M. & Apdillah, D. 2020. Remote sensing of seagrass and seabed using acoustic technology in Bintan Seawater, Indonesia. *Pertanika Journal of Science and Technology* 28(2): 421-439.

Mckenzie, L.J., Nordlund, L.M., Jones, B.L., Cullen-unsworth, L.C., Roelfsema, C. & Unsworth, R.K.F. 2020. The global distribution of seagrass meadows information for data reuse ecosystems. *Environmental Research Letters* 15(7): 158-170.

Medina, J.A.V. & Atehortua, B.E.A. 2018. Comparison of maximum likelihood, support vector machines and random forest techniques in satellite image classification. *Tecnura* 23(59): 13-26.

Mogstad, A.A., Johnsen, G. & Ludvigsen, M. 2019. Shallow-water habitat mapping using underwater hyperspectral imaging from an unmanned surface vehicle: A pilot study. *Remote Sensing* 11(6): 685-699.

Niroumand-Jadidi, M., Pahlevan, N. & Vitti, A. 2019. Mapping substrate types and compositions in shallow streams. *Remote Sensing* 11(3): 262.

Nugraha, A.H., Tasabaramo, I.A., Hernawan, U.E., Rahmawati, S., Putra, R.D. & Darus, R.F. 2021. Diversity, coverage, distribution and ecosystem services of seagrass in three small islands of northern Papua, Indonesia: Liki Island, Meossu Island and Befondi Island. *Biodiversitas* 22(12): 5544-5549.

Nurjirana, Burhanuddin, A.I., Keith, P., Haris, A., Moore, A.M., Afrisal, M., Gani, A., Hasan, V., Wuniarto, E., Bakri, A.A. & Adriany, D.T. 2022. Additional records of *Sicyopus discordipinnis* (Watson, 1995) (Oxudercidae: Sicydiinae) in Central Sulawesi, Indonesia. *Cybium* 46(1): 041-043.

Pardamean, A.L., Islamy, R.A., Hasan, V., Herawati, E.Y. & Mutmainnah, N. 2021. Identification and physiological characteristics of potential indigenous bacteria as bioremediation agent in the wastewater of sugar factory. *Sains Malaysiana* 50(2): 279-286.

Poursanidis, D., Traganos, D., Teixeira, L., Shapiro, A. & Muaves, L. 2021. Cloud-native seascape mapping of Mozambique's Quirimbas National Park with Sentinel-2. *Remote Sensing in Ecology and Conservation* 7(2): 275-291.

Poursanidis, D., Traganos, D., Reinartz, P. & Chrysoulakis, N. 2019. On the use of Sentinel-2 for coastal habitat mapping and satellite-derived bathymetry estimation using downscaled coastal aerosol band. *International Journal of Applied Earth Observation and Geoinformation* 80(1): 58-70.

Prarikeslan, W., Hermon, D., Suasti, Y. & Putra, A. 2019. Density, coverage and biomass of seagrass ecosystem in the Lobam Island, Bintan Regency - Indonesia. *IOP Conference Series: Earth and Environmental Science* 314: 012024.

Rahman, A. 2013. Benthic habitat mapping from seabed images using ensemble of color, texture, and edge features. *International Journal of Computational Intelligence Systems* 6(6): 1072-1081.

Rahman, F.A., Qayim, I. & Wardiatno, Y. 2018. Carbon storage variability in seagrass meadows of Marine Poton Bako, East Lombok, West Nusa Tenggara, Indonesia. *Biodiversitas* 19(5): 1626-1631.

Richards, J.A. & Jia, X. 2006. *Remote Sensing Digital Image Analysis: An Introduction.* Springer. https://doi.org/10.1007/3-540-29711-1

Sabilah, A.A., Siregar, V.P.S. & Amran, M.A. 2021. Comparison of seagrass cover classification based-on SVM and Fuzzy algorithms using multiscale imagery in Kodingareng Lompo Island. *Jurnal Ilmu dan Teknologi Kelautan Tropis* 13(2): 97-112.

Saraswati, S.A., Toruan, L.N.L., Suteja, Y., Karmen, D. & Wijaya, P.E.P. 2021. Rob potential in the coastal city of Kupang, East Nusa Tenggara (NTT). *Journal of Aquaculture and Fish Health* 10(3): 304-311.

Short, F., Carruthers, T., Dennison, W. & Waycott, M. 2007. Global seagrass distribution and diversity: A bioregional model. *Journal of Experimental Marine Biology and Ecology* 350(2): 3-20.

Siregar, V.P., Agus, S.B., Subarno, T. & Prabowo, N.W. 2018. Mapping shallow waters habitats using OBIA by applying several approaches of depth invariant index in North Kepulauan Seribu. *IOP Conference Series: Earth and Environmental Science* 149: 012052. https://doi.org/10.1088/1755-1315/149/1/012052.

Sjafrie, N.D.M., Hernawan, U.E., Prayudha, B., Rahmat, Supriyadi, I.H., Iswari, M.Y., Suyarso, Anggraini, K. & Rahmawati, S. 2018. *Status Padang Lamun*. Pusat Penelitian Oseanografi-LIPI. 53(9).

Supriyadi, I.H., Iswari, M.Y. & Suyarso. 2018. Kajian awal kondisi padang lamun di perairan timur Indonesia. *Jurnal Segara* 14(3): 169-177.

Thalib, M.S., Nurdin, N. & Aris, A. 2018. The ability of Lyzenga's algorithm for seagrass mapping using Sentinel-2A imagery on small island Spermonde Archipelago, Indonesia. *IOP Conference Series: Earth and Environmental Science* 165: 012028. https://doi.org/10.1088/1755-1315/165/1/012028

Traganos, D., Aggarwal, B., Poursanidis, D., Topouzelis, K., Chrysoulakis, N. & Reinartz, P. 2018. Towards global-scale seagrass mapping and monitoring using Sentinel-2 on Google Earth Engine: The case study of the Aegean and Ionian Seas. *Remote Sensing* 10(8): 1-14.

Tzotsos, A. 2006. A support vector machine approach for object based image. *Proceedings of 1st International Conference on Object-Based Image Analysis, Negnevitsky.* pp. 4-15.

Unsworth, R.K.F., Nordlund, L.M. & Cullen-Unsworth, L.C. 2019. Seagrass meadows support global fisheries production. *Conservation Letters* 12(1): 1-8.

Unsworth, R., Ambo-Rappe, R., Jones, B., Nafie, Y., Irawan, A., Hernawan, U.E., Moore, A.M. & Unsworth, L.C. 2018. Indonesia's globally significant seagrass meadows are under widespread threat. *Science of the Total Environment* 634(1): 279-286.

William-Schaduw, J.N. & Ivone Kondoy, K.F. 2020. Seagrass percent cover in small islands of Bunaken National Park, North Sulawesi Province, Indonesia. *AACL Bioflux* 13(2): 951-957.

*Corresponding author; email: zainulhidayah@trunojoyo.ac.id